Dalton Transactions

Accepted Manuscript

This is an *Accepted Manuscript*, which has been through the RSC Publishing peer review process and has been accepted for publication.

Accepted Manuscripts are published online shortly after acceptance, which is prior to technical editing, formatting and proof reading. This free service from RSC Publishing allows authors to make their results available to the community, in citable form, before publication of the edited article. This *Accepted Manuscript* will be replaced by the edited and formatted *Advance Article* as soon as this is available.

To cite this manuscript please use its permanent Digital Object Identifier (DOI®), which is identical for all formats of publication.

More information about *Accepted Manuscripts* can be found in the **Information for Authors**.

Please note that technical editing may introduce minor changes to the text and/or graphics contained in the manuscript submitted by the author(s) which may alter content, and that the standard **Terms & Conditions** and the **ethical guidelines** that apply to the journal are still applicable. In no event shall the RSC be held responsible for any errors or omissions in these *Accepted Manuscript* manuscripts or any consequences arising from the use of any information contained in them.

New Tetrazole-based Cu(I) Homo- and Heteroleptic Complexes with Various Diphosphine Ligands: Synthesis, Characterization and Study of their Redox and Photophysical Properties

Cristina Femoni,[a] Sara Muzzioli,[a] Antonio Palazzi,[a] Stefano Stagni,[a]* Stefano Zacchini,[a] Filippo Monti,[b] Gianluca Accorsi,[b] Margherita Bolognesi,[b] Nicola Armaroli,[b]* Massimiliano Massi,[c] Giovanni Valenti,[d] Massimo Marcaccio[d]

[a]*Dipartimento di Chimica Fisica ed Inorganica, Università di Bologna, Viale Risorgimento 4, I-40136 Bologna, Italy,* e-mail: stefano.stagni@unibo.it

[b]*Molecular Photoscience Group, Istituto per la Sintesi Organica e la Fotoreattività, Consiglio Nazionale delle Ricerche (CNR-ISOF), Via Gobetti 101, I-40129 Bologna*, e-mail: nicola.armaroli@cnr.it

[c]*Department of Chemistry, Curtin University, GPO Box U 1987, Perth, Australia, 6845.*

[d]*Dipartimento di Chimica "G. Ciamician", Università di Bologna, Via Selmi 2, I-40126 Bologna, Italy.*

Abstract

Four Cu(I) complexes with general formulas $[Cu(N\wedge N)_2][BF_4]$ and $[(P\wedge P)Cu(N\wedge N)][BF_4]$ were prepared, where N^N stands for 2-(2-*tert*-butyl-2*H*-tetrazol-5-yl)pyridine and P^P is a chelating diphosphine, namely bis-(diphenylphosphino)methane (dppm), bis-(diphenylphosphino)ethane (dppe) or bis[2-(diphenylphosphino) phenyl]ether (POP). In acetonitrile medium, the Electro-Spray Ionization Mass Spectrometry (ESI-MS) determination provided the preliminary evidence for the occurrence of the dppm-containing complex as a mixture of a cationic mononuclear $[Cu(N^N)(dppm)]^+$ species and a bis cationic dinuclear $[Cu_2(N^N)_2(dppm)_2]^{2+}$-type compound. Definitive evidence of peculiar structural features came from X-ray crystallography, which showed both the dppm- and, unexpectedly, the dppe-based heteroleptic compounds to crystallize as diphosphine-bridged Cu(I) dimers, unlike $[Cu(N^N)_2]^+$ and $[(POP)Cu(N\wedge N)]^+$ which are mononuclear species. In solutions of non-coordinating solvents, ^{31}P NMR studies at variable temperature and dilution titrations confirmed that the dppm-based complex undergoes to a monomer/dimer dynamic equilibrium, while the dppe.-containing complex occurs as the bis-cationic dinuclear species, $[Cu_2(N^N)_2(dppe)_2]^{2+}$, within a concentration range comprised between 10^{-2} and 10^{-4} M.. Differences among heteroleptic complexes might be related the smaller natural bite angle displayed by dppm and dppe phosphine ligands (72° and 85°, respectively), with respect to that reported for POP (102°). The electrochemical features of the new species have been

investigated by cyclic voltammetry. Despite the irreversible and complicated redox behaviour, which is typical for copper complexes, the reductions have been attributed to the tetrazole ligand whereas the oxidations are characterized as Cu(I/II) processes with a substantial contribution from the P^P-based ligands in the case of the heteroleptic species. All the four complexes are weakly or not luminescent in CH_2Cl_2 solution, but heteroleptic complexes are bright green luminophores in solid matrix, with quantum yield as high as 45% (dppm complex) even at room temperature. This makes them potential candidates as cheap emitting materials for electroluminescent devices.

Introduction

The recent developments in the field of Organic Light Emitting Devices (OLEDs) have been promoted and accompanied by considerable research efforts to design and prepare photo- and electroluminescent organic and inorganic compounds exhibiting emission bands all across the visible spectral region.[1] The replacement of "purely" organic emitters with metal complexes in electroluminescent devices has been a key advancement in this area, which resulted in a significant improvement of performance. In fact, the use of complexes of heavy metals allows harvesting of both singlet and triplet excitons, whereas emission from organic luminophores only originates from singlet states.[2] Among the various types of coordination compounds employed as emitters in OLED devices, the "paradigm" is represented by cyclometalated Ir(III) complexes, which can be prepared both as neutral or charged species.[3] The prominent role gained by this class of typically stable Ir(III) derivatives is due to their outstanding photo- and electroluminescent performances, as well as the ease of emission colour tunability via a thorough modification of the ligand environment. Also, well established synthetic procedures are available for the preparation of both neutral and charged luminescent complexes, providing a large variety of Ir(III)-based emitters that can be either directly sublimed into the OLED structure (neutral species) or, as in the case of charged complexes, used in the fabrication of Light Emitting Electrochemical Cells (LEECs) through "wet" methods.[4] Since the most relevant limitation to the use of iridium for lighting technologies is given by its low relative abundance on the Earth's crust and high cost, a great deal of research attention has been recently devoted to find less expensive alternatives.[5] Within this framework, promising results have been obtained with the fabrication of electroluminescent devices where Cu(I) luminescent complexes have been used as emitters in place of the traditional Ir(III) luminophores.[6] In most cases, the Cu(I) species employed for similar purposes were represented by homo or heteroleptic cationic complexes with general formula $[Cu(N\wedge N)_2]^+$, $[(P\wedge P)Cu(N\wedge N)]^+$ or $[Cu(P\wedge P)_2]^+$, where N∧N denotes diimine ligands (e.g. 1,10 phenanthroline) and P∧P represents chelating diphosphines.[7] As far as P^P–type ligands are concerned, a wide range of aromatic diphosphines such as bis-(diphenylphosphino)methane (dppm) and bis-(diphenylphosphino)ethane (dppe, as represented in Scheme 1) or similar molecules, have been employed so far and, among the many examples reported in the literature, bis[2-(diphenylphosphino) phenyl]ether, denoted as DPEphos or POP, has gained a prominent role for the design of Cu(I) complexes.[6f-g,7,8] Aiming at further widening the family of photoactive Cu(I) complexes, herein we report about the synthesis, the characterization and the study of the photophysical properties of a set of new cationic Cu(I) complexes consisting of one homoleptic $[Cu(N\wedge N)_2]^+$-type compound and three heteroleptic $[(P\wedge P)Cu(N\wedge N)]^+$ derivatives

(Scheme 1), where N∧N is 2-(2-*tert*-butyl-2*H*-tetrazol-5-yl)pyridine and P^P is a chelating diphosphine. The element of novelty in the present work is given by the use of a tetrazole derivative as the diimine N∧N ligand. The use of these nitrogen-rich ligands further develops our previous studies where aromatic 5-substituted tetrazolates were reported as excellent and versatile components for the design of photo and electroluminescent Ru(II)-polypyridines,[9] Ir(III) cyclometalates,[4b,10] and Re(I) diimine complexes.[11]

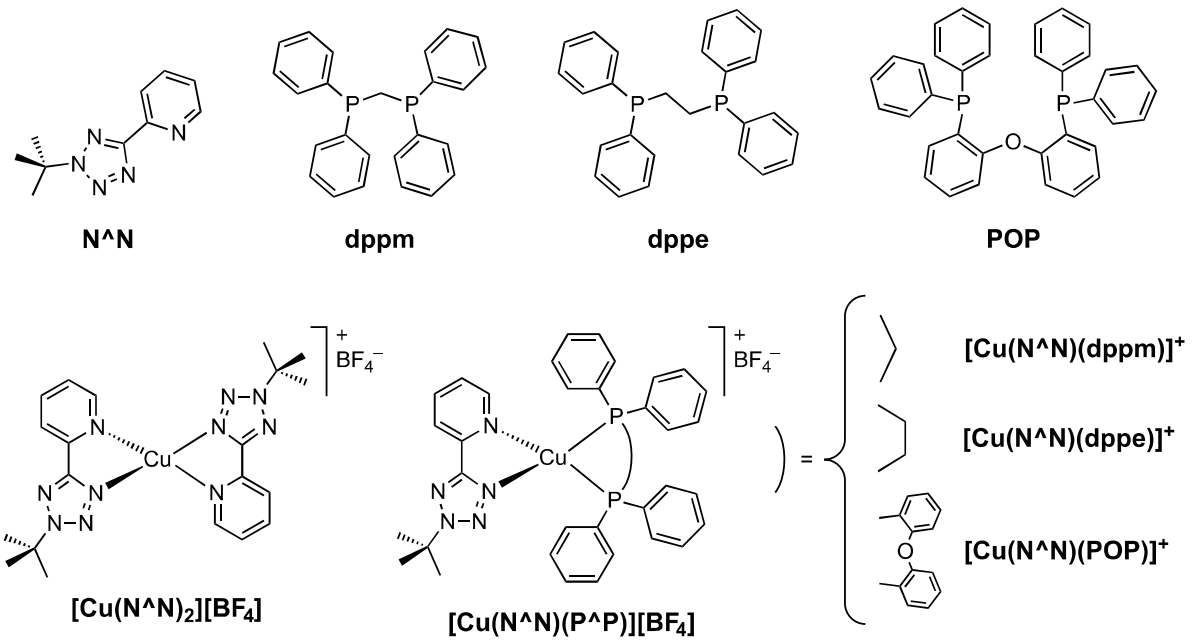

Scheme 1. Ligands, complexes and acronyms

Results and discussion

Synthesis

The choice of using a N-alkylated tetrazole derivative as the N^N diimine type ligand, in place of an acidic N-H tetrazole, is mainly due to the better solubility exhibited by these compounds in most of the common organic solvents. The alkylated tetrazole, N^N, was prepared according to a reported procedure[12] involving the reaction of the starting N-H tetrazole with *tert*-butyl alcohol in the presence of H_2SO_4 and CF_3COOH. By following this synthetic method (Scheme 2), the regioselective formation of the desired N-2 *tert*-butyl tetrazole derivative was achieved, whereas the use of less sterically demanding alkyl fragments would lead to the formation of inseparable mixtures of N-1 and N-2 alkylated products.

The preparation of all the Cu(I) complexes has been accomplished according to literature methods.[8] In particular, the homoleptic species was straightforwardly obtained from the addition of two molar

equivalents of the N∧N ligand to a dichloromethane solution of $[Cu(CH_3CN)_4][BF_4]$, [13] whereas the formation of heteroleptic compounds required a two-steps procedure involving the preliminary reaction of $[Cu(CH_3CN)_4][BF_4]$ with a 1 molar equivalent of diphosphine P∧P, followed by the addition of the N^N ligand (Scheme 2). Among the four new complexes, all of which were recovered as their tetrafluoroborate salts, a pronounced oxygen sensitivity, leading to quite fast Cu(I) oxidation, was displayed by the homoleptic compound $[Cu(N^N)_2]^+$ and, to a lesser extent, by the dppm-contaning complex $[Cu(N^N)(dppm)]^+$. The remaining compounds $[Cu(N^N)(POP)]^+$ and $[Cu(N^N)(dppe)]^+$ were found to be air-stable.

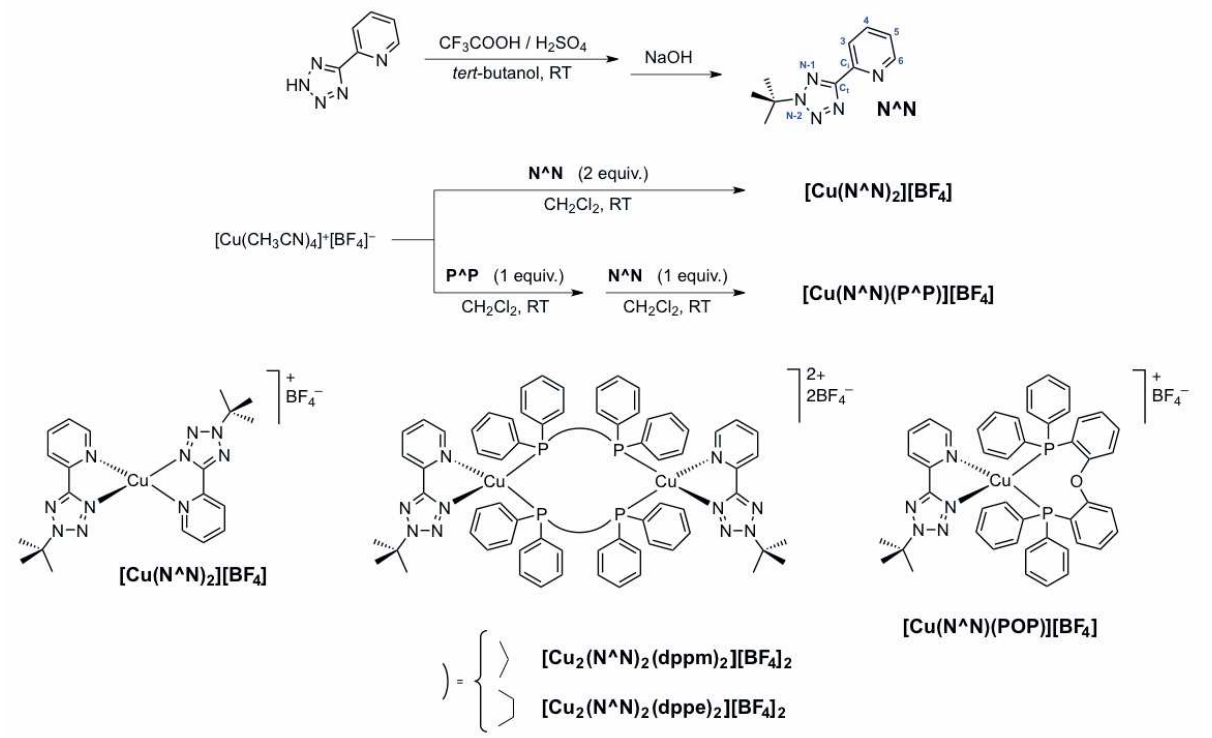

Scheme 2. Synthetic procedure for the preparation of the ligand N^N and all of the Cu(I) complexes

Characterization

The complexes were at first characterized by Electro-Spray Ionization Mass Spectrometry (ESI-MS) spectrometry in acetonitrile. The observed molecular ion peaks, as well as their corresponding isotopic distributions, were consistent with the expected mononuclear cationic complexes in almost all cases, the only discrepancy being the heteroleptic dppm-containing cation $[Cu(N^N)(dppm)]^+$. In this latter case, indeed, the preliminary evidence for the formation of a bis-cationic dinuclear complex was provided by the presence, in the positive ions ESI-MS spectrum (Figs. S2 and S4, Supporting information), of a signal centered at 550 *m/z*, which is likely attributable to the loss of one N^N ligand from the dinuclear $[Cu_2(N^N)_2(dppm)_2]^{2+}$ species. Also, the distribution of the isotopic pattern of the molecular ion peak centered at 650 *m/z* does not match neither the mononuclear complex nor the dinuclear one, but it rather suggests the presence of a mixture of the two species, as also deduced from the analysis of high-resolution ESI- MS spectra. (Figs. S2 and S3, Supporting Information).

The (^1H, ^{13}C and ^{31}P) NMR characterization of all the new complexes indicated the formation of the expected homoleptic and heteroleptic species, even though appreciably resolved ^1H NMR spectra of the dppm-containing species could be obtained only at T= 233 K (see Fig.S11, Supporting Information). In particular, the structural assignment of the mixed ligand complexes was confirmed by the presence, in their ^{31}P spectra, of one sharp singlet resonating in the chemical shifts range comprised between -4.3 (for $[Cu(N^N)(dppe)]^+$), -6.9 (for $[Cu(N^N)(dppm)]^+$), and -11.2 ppm (for complex $[Cu(N^N)(POP)]^+$). However, as we were able to obtain single crystal X-ray diffraction data for all the complexes, it was possible to further circumstantiate the assignments made on the basis of NMR and ESI-MS data. In particular, as described in detail in the following section, it was observed that the complexes $[Cu(N^N)_2]^+$ and $[Cu(N^N)(POP)]^+$ crystallized as the expected mononuclear species, while the dppm- and the dppe-based heteroleptic compounds crystallized as diphosphine-bridged Cu(I) dimers like $[Cu_2(N^N)_2(dppm)_2]^{2+}$ and $[Cu_2(N^N)_2(dppe)_2]^{2+}$, respectively, the formation of which might be at a glance and tentatively explained by considering the smaller natural bite angle displayed by dppm and dppe (72° and 85°, respectively)[14], with respect to that reported for the POP ligand (102°).[14,15] Nevertheless, whereas the interpretation of the data obtained from ESI-MS characterization anticipated the occurrence of a similar feature for the dppm-containing complex, the formation of the dppe-bridged Cu(I)-based dimer $[Cu_2(N^N)_2(dppe)_2]^{2+}$ was less expected.

In order to gain more insight about the behaviour of the new heteroleptic compounds and better understand the nature of the predominant species in solutions of non-coordinating solvents, some further ^{31}P NMR studies were performed onto all the mixed ligand complexes by means of variable

temperature (VT) experiments together with dilution titrations. Concerning VT ^{31}P NMR experiments in $CDCl_3$, no appreciable variations have been detected for $[Cu(N^N)(POP)]^+$ and $[Cu(N^N)(dppe)]^+$ between room temperature and 233 K (Figs. S15 and S8 in Supporting Information, respectively), while substantial changes were observed in the case of the Cu(I)-dppm derivative. (Fig. 1) Indeed, upon cooling to 233 K, the singlet centred at ca. -7.0 ppm splits into two closely spaced signals, with coalescence observed between 273 and 268 K. A similar effect might be ascribed to the stabilization of magnetically not-equivalent phosphorus atoms of the strained $Cu_2C_2P_4$ cage displayed by the crystal structure of the complex in its dimeric form $[Cu_2(N^N)_2(dppm)_2]^{2+}$ (see next section). This assignment is also suggested by the analysis of the dilution ^{31}P NMR titrations performed at the same temperatures onto a raw sample of the dppm-containing complex obtained by dissolving 22.0 mg of the compound in 0.75 mL of $CDCl_3$. At room temperature, (Fig. 1, left) the resulting ^{31}P NMR spectrum consists of a well resolved singlet centered at -7.0 ppm accompanied by a much smaller signal which resonates at -13.90 ppm. The integral ratio of the two different signals is 1/0.03. Upon performing a ten-fold dilution of the sample, the integral of the signal centered at -13.90 ppm increases and the integral ratio becomes 1/0.17, while the two signals have an almost equivalent integral value (1/0.78) as the concentration is further reduced by a factor of ten. By assuming the species $[Cu_n(N^N)_n(dppm)_n]^{n+}$(n=1,2) as being involved in a dimer-monomer equilibrium of the type $A_2 \leftrightarrow 2A$, such a concentration-dependent behaviour might be explained by the gradual formation, over the course of dilution, of the monomer 2A-type species that arise from the dissociation of the dimeric one (A_2), that is likely predominant at higher concentration.

The same behaviour is observed by performing the dilution experiments onto samples measured at -40°C (233.15 K). (Fig. 1, right)

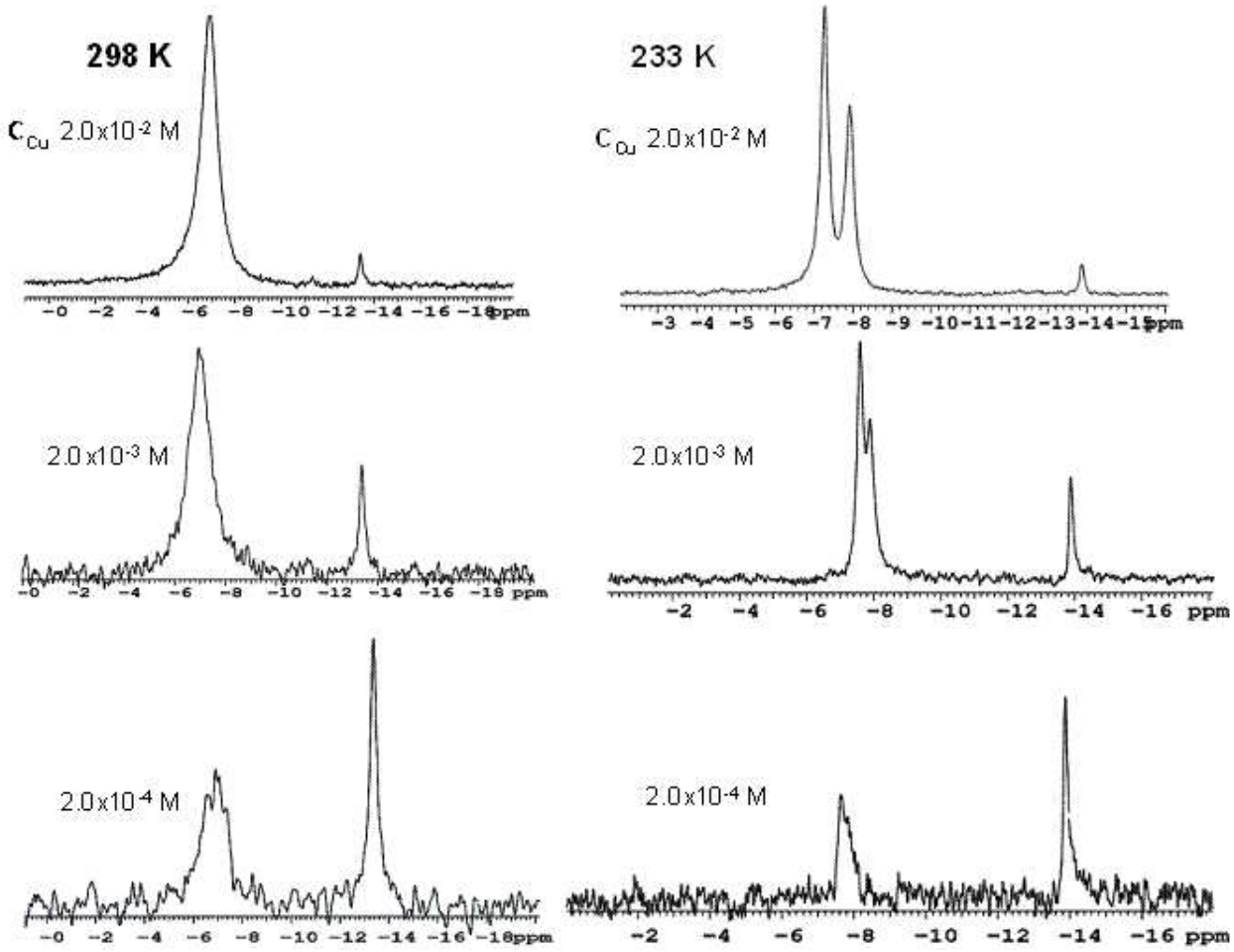

Fig. 1. Stacking plot of ^{31}P NMR spectra ($CDCl_3$ as the solvent) of the dppm containing Cu complex. at different concentration at 298 K (left) and at 233 K (right). The concentration values (C_{Cu}) are calculated by considering the dinuclear species $[Cu_2(N\hat{}N)_2(dppm)_2][BF_4]_2$ [F.W.= 1475 g/mol] as the prevalent one in each starting experiment.

A totally different behaviour was displayed by dppe-based mixed ligand complex, which was found to crystallize in a dimeric fashion adopting a chair-type ten-membered $Cu_2P_4C_4$ ring. In this case, the successive dilutions of the sample did not result in any change of its ^{31}PNMR spectrum, which invariably displayed one singlet resonating at ca. -4.30 ppm (Fig.S9, Supporting Information). Taken together these results suggest that in solutions of non-coordinating solvents the distribution of the heteroleptic complex $[Cu_n(N\hat{}N)_n(dppm)_n]^{n+}$ (n=1,2) between the cationic momomer (n=1) and the corresponding dicationic dimer (n=2) is ruled by a concentration-dependent equilibrium that involves the prevalence of the dimeric form for concentration values up to *ca.* 10^{-3} M. On the other hand, the likely exclusive speciation of the dppe-based as the dinuclear dimer $[Cu_2(N\hat{}N)_2(dppe)_2]^{2+}$ is observed within the same concentration limits (10^{-2} to 10^{-4} M) that were considered for the study

of the dppm-containing complex. The coordinating character of the solvent is of crucial importance for determining the nuclearity of the species in solution, as confirmed by the ESI-MS spectrum of an acetonitrile solution of the crystals of $[Cu_2(N^N)_2(dppe)_2]^{2+}$ that were used for X-ray diffraction analysis. Such spectrum displayed the molecular ion peak with an isotopic distribution pattern consistent with mononuclear species (Fig. S1, Supporting Information) and further ^{31}P NMR dilution titrations performed both on the dppm (Fig. S13, Supporting Information) and on the dppe (Fig S10, Supporting Information) mixed complexes in CD_3CN resulted in spectra where no growth of further signals was observed.

Crystal structures

The structures of the $[Cu(N^N)_2]^+$ (Fig. 2 and Table 1), $[Cu_2(N^N)_2(dppm)_2]^{2+}$ (Fig. 3 and Table 2), $[Cu_2(N^N)_2(dppe)_2]^{2+}$ (Fig. 4 and Table 3) and $[Cu(N^N)(POP)]^+$ (Fig. 5 and Table 4) cationic complexes have been determined in their $[Cu(N^N)_2][BF_4]$, $[Cu_2(N^N)_2(dppm)_2][BF_4]_2$, $[Cu_2(N^N)_2(dppe)_2][BF_4]_2{\cdot}Et_2O$ and $[Cu(N^N)(POP)][BF_4]{\cdot}Et_2O$ salts. It must be remarked that $[Cu(N^N)_2]^+$ and $[Cu(N^N)(POP)]^+$ display monomeric structures, whereas both $[Cu_2(N^N)_2(dppm)_2]^{2+}$ and $[Cu_2(N^N)_2(dppe)_2]^{2+}$ are dinuclear complexes. The Cu(I) centre in the homoleptic $[Cu(N^N)_2]^+$ cation (Fig. 1 and Table 1) adopts a distorted tetrahedral geometry as consequence of the small bite angles of the two chelating pyridyl tetrazole ligands [N(1)-Cu(1)-N(5) 81.90(7)°; N(6)-Cu(1)-N(10) 82.04(7)°]. The solid state structure confirms that the tetrazole ring is alkylated on N(3) and coordinate to Cu(1) *via* N(1). Both pyridyl tetrazole ligands are almost perfectly planar [mean deviations from the least squares planes comprising the tetrazole and pyridyl rings 0.0634 and 0.0318 Å for the two N^N ligands, respectively] and their planes are nearly orthogonal [82.8 °]. The Cu-N(tetrazole) [Cu(1)-N(1) 2.0136(17) Å; Cu(1)-N(6) 2.0353(17) Å] and Cu-N(pyridine) [Cu(1)-N(5) 2.0557(16) Å; Cu(1)-N(10) 2.0262(18) Å] are very similar since both N-atoms belong to neutral aromatic rings.

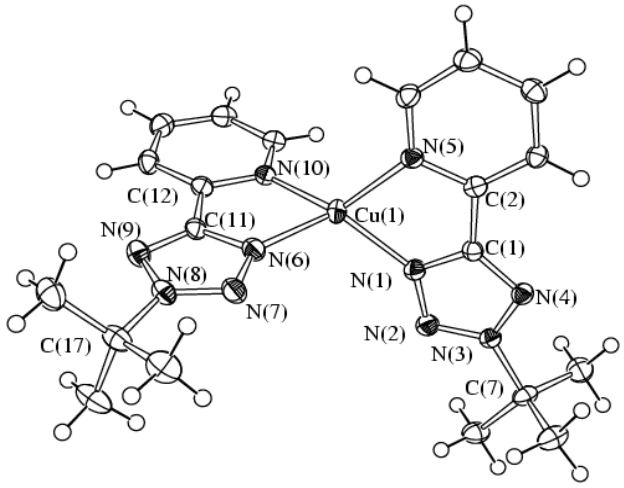

Fig. 2. Molecular structure of the cation $[Cu(N^N)_2]^+$ with key atoms labelled. Displacement ellipsoids are at 20 %. probability level.

Table 1. *Selected Bond Lengths (Å) and Angles (deg) for* $[Cu(N^N)_2]^+$.

Cu(1)-N(1)	2.0136(17)	Cu(1)-N(6)	2.0353(17)
Cu(1)-N(5)	2.0557(16)	Cu(1)-N(10)	2.0262(18)
N(1)-N(2)	1.318(2)	N(6)-N(7)	1.324(2)
N(2)-N(3)	1.317(2)	N(7)-N(8)	1.321(2)
N(3)-N(4)	1.332(2)	N(8)-N(9)	1.345(3)
C(1)-N(1)	1.346(3)	C(11)-N(6)	1.353(3)
C(1)-N(4)	1.331(3)	C(11)-N(9)	1.322(3)
N(3)-C(7)	1.496(2)	N(8)-C(17)	1.489(3)
C(1)-C(2)	1.469(3)	C(11)-C(12)	1.461(3)
C(2)-N(5)	1.353(3)	C(12)-N(10)	1.355(3)
N(1)-Cu(1)-N(5)	81.90(7)	N(6)-Cu(1)-N(10)	82.04(7)
C(1)-N(1)-N(2)	106.88(16)	C(11)-N(6)-N(7)	106.87(16)
N(1)-N(2)-N(3)	105.30(16)	N(6)-N(7)-N(8)	105.34(17)
N(2)-N(3)-N(4)	114.60(16)	N(7)-N(8)-N(9)	114.07(16)
N(3)-N(4)-C(1)	101.12(16)	N(8)-N(9)-C(11)	101.54(17)
N(1)-C(1)-N(4)	112.10(17)	N(6)-C(11)-N(9)	112.19(19)

Unlike homoleptic $[Cu(N^N)_2]^+$, the heteroleptic compounds containing N^N and dppm or dppe display in the solid state a dinuclear structure (see above for the discussion of their nature in solution as determined via VT NMR studies). The structure of the dimeric $[Cu_2(N^N)_2(dppm)_2]^{2+}$ dication is depicted in Fig. 2 whereas its most relevant bonding parameters are reported in Table 2. The two Cu(I) centres show also in this case a distorted tetrahedral geometry, both being coordinated to a chelating pyridyl tetrazole N^N ligand and to two P-atoms of two different bridging dppm ligands. The bite angle of the chelating N^N ligand in this dinuclear heteroleptic compound [N(1)-Cu(1)-N(5) 77.99(16)°; N(6)-Cu(2)-N(10) 78.31(17)°] is very similar to the ones found in mononuclear homoleptic $[Cu(N^N)_2]^+$, and also in this case the pyridine and tetrazole rings of the N^N ligand are almost coplanar [mean deviations from the least squares planes 0.0307 and 0.0562 Å for Å for the two N^N ligands, respectively], as a consequence of its chelating behaviour. The P-Cu-P angles [P(1)-Cu(1)-P(3) 139.20(5)°; P(2)-Cu(2)-P(4) 137.71(5)°] are comparable to those found in analogous complexes $[Cu_2(N^N)_2(dppm)_2]^{2+}$ (N^N = substituted phenantroline or bipyridine) containing two bridging dppm and chelating N^N ligands.[16]

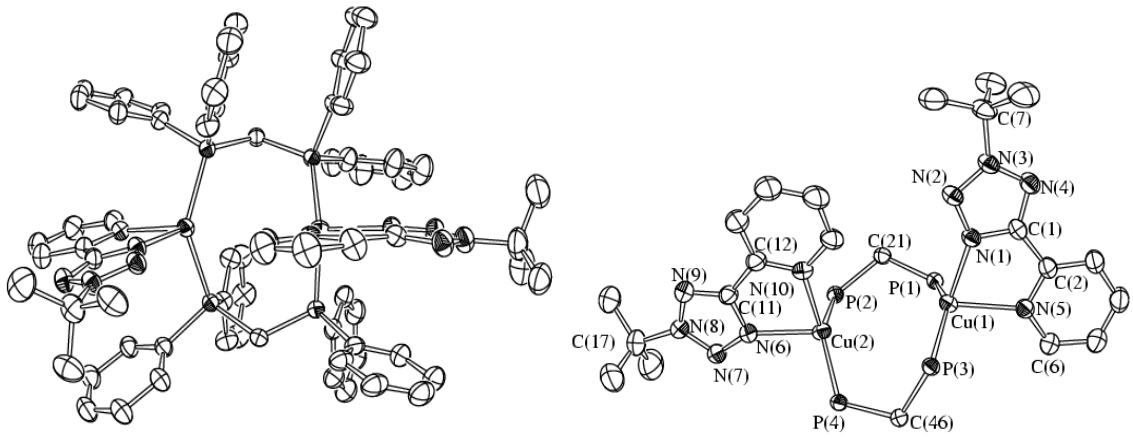

(a) (b)

Fig. 3. Molecular structure of the dication $[Cu_2(N^N)_2(dppm)_2]^{2+}$: (a) view of the complete structure (H-atom omitted for clarity); (b) labelling scheme (Ph rings omitted). Displacement ellipsoids are at 30 % probability level.

Table 2. Selected Bond Lengths (Å) and Angles (deg) for $[Cu_2(N^N)_2(dppm)_2]^{2+}$.

Cu(1)-N(1)	2.079(4)	Cu(2)-N(6)	2.147(4)
Cu(1)-N(5)	2.218(4)	Cu(2)-N(10)	2.128(4)
Cu(1)-P(1)	2.2861(14)	Cu(2)-P)2)	2.2527(14)
Cu(1)-P(3)	2.2440(13)	Cu(2)-P(4)	2.2259(13)
N(1)-N(2)	1.313(6)	N(6)-N(7)	1.311(6)
N(2)-N(3)	1.323(6)	N(7)-N(8)	1.313(6)
N(3)-N(4)	1.326(6)	N(8)-N(9)	1.332(7)
C(1)-N(1)	1.352(6)	C(11)-N(6)	1.352(6)
C(1)-N(4)	1.321(6)	C(11)-N(9)	1.322(7)
N(3)-C(7)	1.489(7)	N(8)-C(17)	1.498(8)
C(1)-C(2)	1.460(7)	C(11)-C(12)	1.457(8)
C(2)-N(5)	1.343(6)	C(12)-N(10)	1.348(7)
P(1)-C(21)	1.845(5)	P(2)-C(21)	1.826(5)
P(3)-C(46)	1.837(5)	P(4)-C(46)	1.835(5)
N(1)-Cu(1)-N(5)	77.99(16)	N(6)-Cu(2)-N(10)	78.31(17)
C(1)-N(1)-N(2)	107.0(4)	C(11)-N(6)-N(7)	107.0(4)
N(1)-N(2)-N(3)	105.2(4)	N(6)-N(7)-N(8)	105.7(4)
N(2)-N(3)-N(4)	114.2(4)	N(7)-N(8)-N(9)	114.0(5)
N(3)-N(4)-C(1)	101.9(4)	N(8)-N(9)-C(11)	101.9(4)
N(1)-C(1)-N(4)	111.7(5)	N(6)-C(11)-N(9)	111.4(5)
P(1)-Cu(1)-P(3)	139.20(5)	P(2)-Cu(2)-P(4)	137.71(5)
P(1)-C(21)-P(2)	114.9(2)	P(3)-C(46)-P(4)	113.6(2)
Cu(1)-P(1)-C(21)	123.72(16)	Cu(2)-P(2)-C(21)	113.65(17)
Cu(1)-P(3)-C(46)	116.89(16)	Cu(2)-P(4)-C(46)	121.59(16)

The centrosymmetric structure of the dinuclear $[Cu_2(N^N)_2(dppe)_2]^{2+}$ complex is illustrated in Fig. 3 and its most relevant bonding parameters are reported in Table 3. As shown below, the two Cu atoms are doubly bridged by two dppe ligands to form a ten-membered $Cu_2P_4C_4$ ring arranged in a chair conformation. This has already been observed for similar dinuclear complexes when two dppe ligands are coordinated to two different Cu(I) atoms which, in turn, are bonded to chelating molecules.[17] On the other hand, according to the reports that have appeared in the literature, all of the structurally similar $[Cu(N^N)(dppe)]^+$-like species (where N^N denotes aromatic diimine

ligands) were shown to crystallize as mononuclear compounds.[18] In addition, relative to a series of $[Cu(dmp)(Ph_2P(CH_2)_nPPh_2)]^+$ (n = 2-5, dmp is 2,9-dimethyl-1,10-phenantroline) type complexes, the formation of dimeric structures was observed only for the dppb-derivative (n=4).[19] However, in agreement with what observed for the previous mono- and dinuclear species, both Cu(I) centres possess a distorted tetrahedral geometry, mainly due to the small bite angle entailed by the pyridyl tetrazole ligand (N(1)-Cu(1)-N(11) = 79.47(2)°). The P(2)-Cu(1)-P(3) angles are closer to the ones required by the tetrahedral geometry, being both 113.80(2)°. Importantly, this value is perfectly in line with the ones found in the mononuclear $[Cu(N^N)(POP)]^+$ derivative and reported in the literature for analogous dinuclear Cu complexes,[17] although noticeably wider than the P-Cu-P angles (ca. 92-93°) that are displayed by the molecular structures of the previously reported mononuclear $[Cu(N^N)(dppe)]^+$-type derivatives.[18] The Cu-N(tetrazole) and Cu-N(pyridine) bond distances (2.108(5) and 2.096(9) Å, respectively) are comparable with the ones found in the $[Cu(N^N)_2]^+$ cation. Likewise, the N-P(dppe) bond lengths (2.251(6) and 2.273(6) Å) do not significantly differ from those observed in the dinuclear $[Cu_2(N^N)_2(dppm)_2]^{2+}$ and mononuclear $[Cu(N^N)(POP)]^+$ complexes.

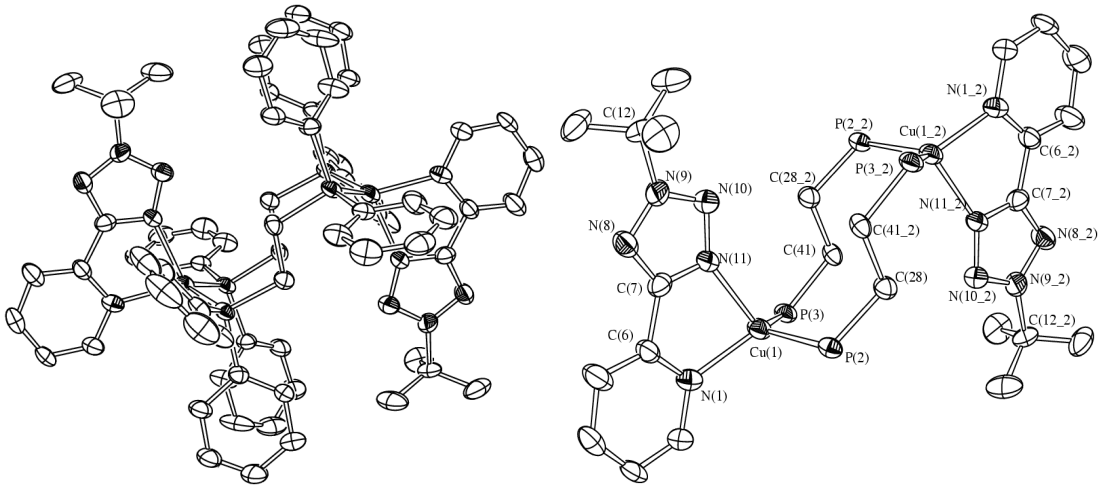

(a) (b)

Fig. 4. Molecular structure of the $[Cu_2(N^N)_2(dppe)_2]^{2+}$ dication: (a) view of the complete structure (H-atom omitted for clarity); (b) labelling scheme (Ph rings omitted). Displacement ellipsoids are at 30 % probability level.

Table 3. Selected Bond Lengths (Å) and Angles (deg) for $[Cu_2(N^N)_2(dppe)_2]^{2+}$.

Cu(1)-N(1)	2.096(8)	N(9)-C(12)	1.526(11)
Cu(1)-N(11)	2.108(8)	N(10)-N(11)	1.354(9)
Cu(1)-P(3)	2.251(3)	P(2)-C(22)	1.801(9)
Cu(1)-P(2)	2.273(3)	P(2)-C(16)	1.840(10)
N(1)-C(6)	1.341(11)	P(2)-C(28)	1.865(8)
C(6)-C(7)	1.490(12)	C(28)-C(41)_1	1.560(10)
C(7)-N(8)	1.336(10)	P(3)-C(35)	1.843(9)
C(7)-N(11)	1.346(10)	P(3)-C(29)	1.856(10)
N(8)-N(9)	1.340(9)	P(3)-C(41)	1.858(8)
N(9)-N(10)	1.330(9)	C(41)-C(28)_1	1.560(10)
N(1)-Cu(1)-N(11)	79.5(3)	C(7)-N(8)-N(9)	100.4(8)
N(1)-Cu(1)-P(3)	122.6(2)	N(10)-N(9)-N(8)	114.6(8)
N(11)-Cu(1)-P(3)	114.8(2)	N(10)-N(9)-C(12)	123.3(9)
N(1)-Cu(1)-P(2)	111.7(2)	N(8)-N(9)-C(12)	121.6(9)
N(11)-Cu(1)-P(2)	109.4(2)	N(9)-N(10)-N(11)	105.7(7)
P(3)-Cu(1)-P(2)	113.80(11)	C(7)-N(11)-N(10)	104.7(8)
C(6)-N(1)-C(2)	114.3(8)	C(7)-N(11)-Cu(1)	111.0(6)
C(6)-N(1)-Cu(1)	116.0(6)	N(10)-N(11)-Cu(1)	143.2(7)
N(8)-C(7)-N(11)	114.5(8)	C(28)-P(2)-Cu(1)	113.1(3)
N(8)-C(7)-C(6)	125.0(10)	C(41)_1-C(28)-P(2)	107.7(5)
N(11)-C(7)-C(6)	120.5(9)	C(41)-P(3)-Cu(1)	111.0(3)

Unlike the above mentioned $[Cu_2(N^N)_2(dppm)_2]^{2+}$ and $[Cu_2(N^N)_2(dppe)_2]^{2+}$ dinuclear compounds, the POP derivative $[Cu(N^N)(POP)]^+$ is mononuclear in the solid state (Fig. 5 and Table 4). Several mononuclear $[Cu(N^N)(POP)]^+$ (N^N = substituted phenantroline or bipyridine) are known and all display structures closely related to the herein described compound where N^N = pyridyl tetrazole.[8,20] The Cu(1) centre displays a distorted tetrahedral geometry as in all the compounds reported in this paper and also the N^N bite angle is very similar [N(1)-Cu(1)-N(5) 78.6(2)°]. The P(1)-Cu(1)-P(2) angle [114.34(6)°] is in the usual range for a chelating POP ligand, which normally displays a rather large natural bite angle.[14,15]

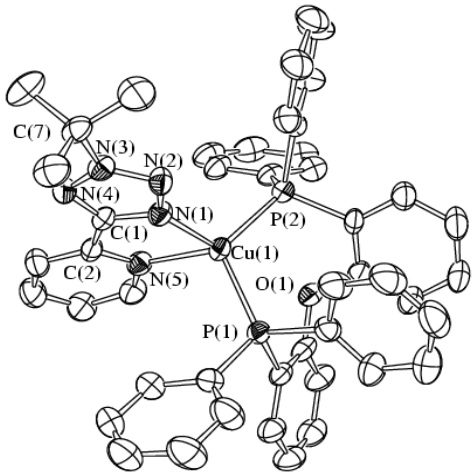

Fig. 5. Molecular structure of the cation $[Cu(N^N)(POP)]^+$ with key atoms labelled. H-atoms have been omitted for clarity. Displacement ellipsoids are at 30 % probability level.

Table 4. Selected Bond Lengths (Å) and Angles (deg) for $[Cu(N^N)(POP)]^+$.

Cu(1)-N(1)	2.093(5)	Cu(1)-N(5)	2.129(6)
Cu(1)-P(1)	2.2628(17)	Cu(1)-P(2)	2.2361(18)
N(1)-N(2)	1.309(7)	N(2)-N(3)	1.321(7)
N(3)-N(4)	1.325(7)	N(3)-C(7)	1.520(8)
C(1)-N(1)	1.342(8)	C(1)-N(4)	1.331(8)
C(1)-C(2)	1.454(10)	C(2)-N(5)	1.348(8)
N(1)-Cu(1)-N(5)	78.6(2)	P(1)-Cu(1)-P(2)	114.34(6)
C(1)-N(1)-N(2)	108.3(5)	N(1)-N(2)-N(3)	104.2(5)
N(2)-N(3)-N(4)	115.0(5)	N(3)-N(4)-C(1)	101.4(5)
N(1)-C(1)-N(4)	111.1(6)		

Redox and Electronic Properties

The electrochemical behaviour of the complexes was investigated in dichloromethane by cyclic voltammetry (CV) at room temperature, using platinum disk as working electrode, and the redox potentials of the various processes are collected in Table 5. The cyclic voltammetric curves of the homoleptic complex $[Cu(N^N)_2]^+$ and the heteroleptic species $[Cu_n(N^N)_n(dppm)_n]^{n+}$ (n=1,2), $[Cu_2(N^N)_2(dppe)_2]^{2+}$ and $[Cu(N^N)(POP)]^+$ are reported in Fig. 6.

Table 5. Redox Potentials[a] (vs SCE) of all Complexes at 25 °C

Species	(*Ox.*) - E_{ox} / V		(*Red.*) - E_{red}/ V	
	(1)	(2)	(1)	(2)
$[Cu(N^N)_2]^+$	0.72[b]	--	-0.73[b]	--
$[Cu_n(N^N)_n(dppm)_n]^{n+}$ (n=1,2)[e]	1.55[c]	1.84[c]	-1.80[c]	-1.96[c]
$[Cu_2(N^N)_2(dppe)_2]^{2+}$	1.06[c]	1.21[c]	-1.93[c]	--
$[Cu(N^N)(POP)]^+$	1.31[d]	1.65[c]	-1.96[c]	--

[a] In a 0.08 M $TBAPF_6$/DCM solution.
[b] Sluggish electrochemical process. $E_{1/2}$ value obtained by digital simulation of the experimental voltammetric curves.
[c] Irreversible process; peak potential measured at 1 V/s.
[d] $E_{1/2}$ potential value
[e] Monomer/dimer mixture species (see discussion)

As a preliminary consideration, it should be noted that, according to the interpretation of the ^{31}P NMR data and to the analysis of the X-ray crystal structures (see previous sections), at the concentration used for the voltammetric investigations (comprised between 0.5 and 0.9 mM), the three heteroleptic complexes were found either as mononuclear (i.e. $[Cu(N^N)(POP)]^+$) or dinuclear (as for $[Cu_2(N^N)_2(dppe)_2]^{2+}$) or as a dimer/monomer (integral ratio (^{31}P NMR): 1/0.17, corresponding to a molar ratio of *ca.* 3/1) mixture for the dppm-based complex $[Cu_n(N^N)_n(dppm)_n]^{n+}$ (n=1,2).

In general, the interpretation of the redox features of all the new Cu(I) complexes was complicated by the electrochemical and chemical irreversible character of the redox processes. However, by the comparison of the voltammetric curves of the homoleptic complex and of all the other heteroleptic systems, it is possible to tentatively assign the redox processes that are found both in the positive and in the negative potentials region of the voltammetric curves. In particular, the two cycles CV of the homoleptic species $[Cu(N^N)_2]^+$ shows two one-electron transfers (Fig. 6a): a ligand (N^N) based reduction process and a Cu(I)-centered oxidation one. Both processes are irreversible and it is worth noting that an intense adsorption spike can be observed, on the second voltammetric cycle, as a consequence of having performed the reduction, thus suggesting that the reduced form of

$[Cu(N^N)_2]^+$ is strongly adsorbed on the electrode. The analysis of both processes indicated that they are sluggish electron transfers and the potentials $E_{½}$ of -0.73 V (*vs* SCE) for the reduction and +0.72 V (vs SCE) for the oxidation have been obtained by digital simulation of the voltammetric curves, with heterogeneous constants of $0.7\pm0.2\cdot10^{-3}$ cm/s and $1.0\pm0.2\cdot10^{-3}$ cm/s, respectively. Moreover, severe surface effects influence the morphology of the voltammetric curves. In fact, on the second cycle of both CVs (the red curve and the black one of Fig. 6a) there is a sizeable shift of the peak potentials. The replacement of the N^N ligand with one P^P unit yielded substantial differences in the voltammograms of the mixed ligand $[Cu_n(N^N)_n(P^P)_n]^{n+}$ (n=1,2) complexes with respect to the case of the homoleptic one $[Cu(N^N)_2]^+$. Indeed, in agreement with previous reports dealing with similar Cu(I) species,[6e-f, 7a, 8c] two distinct processes are observed in the positive potential side of their voltammetric curves, while one or, as in the case of the dppm-based species, two likely N^N centred reductions are present in the cathodic region..

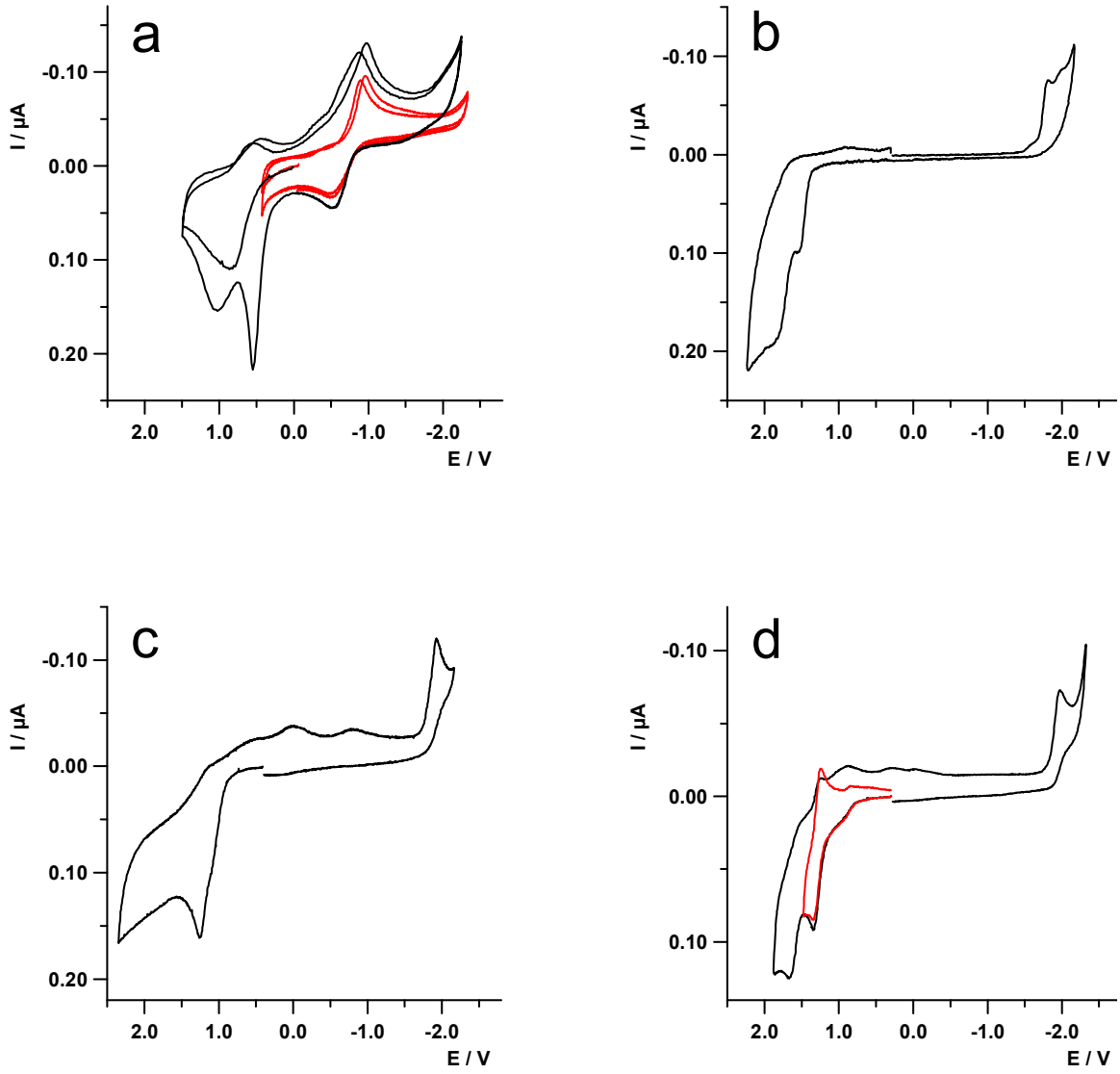

Fig. 6. Cyclic voltammetric curves of species (a) $[Cu(N^N)_2]^+$ 0.9 mM, (b) $[Cu_n(N^N)_n(dppm)_n]^{n+}$ (n=1,2) 0.5 mM, (c) $[Cu_2(N^N)_2(dppe)_2]^{2+}$ 0.5 mM and (d) $[Cu(N^N)(POP)]^+$ 0.9 mM in 0.08 M TBAH/DCM solution. Sweep rate 1 V/s; working electrode: Pt (125 µm, diameter); T=25 °C.

The comparison of the redox potentials between the heteroleptic complexes and the homoleptic one shows a shift of 300-800 mV toward more positive potentials for the oxidation and a much larger shift (> 1V) toward more negative potentials for the reduction. This is consistent with the differences in the electronic properties of the ligands (diphosphines replacing one of the pyridyl-tetrazoles). As mentioned before, each mixed ligand complex displays two redox processes in the anodic region. According to previous reports,[6f,7a] the first process is assigned to the oxidation of the Cu(I) metal centre, while that occurring at more positive potentials is localized on the chelating P^P

ligand. Apart from the first oxidation of $[Cu(N^N)(POP)]^+$, these processes are irreversible in all the mixed ligand species $[Cu_n(N^N)_n(P^P)_n]^+$ (n = 1,2) and, in general, no particular evidence for the different speciation of these compounds can be determined from the analysis of the region of the positive potentials of the corresponding voltammograms (Figs. 6b-d).

In this regard, the indications that might be deduced from the comparison of the voltammetric curves in the side of the negative potentials are only partial and not fully decisive. Indeed, the predominantly dimeric complex $[Cu_n(N^N)_n(dppm)_n]^{n+}$ (n=1,2) displays an irreversible reduction process followed by a smaller peak, also irreversible, at the onset of the solvent/electrolyte discharge. In principle, two successive reductions of the dimeric $[Cu_2(N^N)_2(dppm)_2]^{2+}$ complex should be expected. However, it has to be pointed out that the second process, the one occurring at more negative potentials, is approximately one fifth of the first peak (Fig. 6b). A similar behaviour might be also consistent with the reductions of both the dimeric and the monomeric species that, according to NMR evidences, are present in 3/1 molar ratio, and are involved into the concentration dependent monomer dimer equilibrium that has been described above The interpretation of this voltammetric picture is not helped by the comparison with the voltammogram of $[Cu_2(N^N)_2(dppe)_2]^{2+}$ (Fig 6c). Indeed, this dimeric species exhibits one single and irreversible reduction peak, giving rise to a voltammetric pattern that is quite similar to that of the monomeric complex $[Cu(N^N)(POP)]^+$ (Fig. 6d and Table 5).

Electronic spectra – Excited state properties

The electronic absorption spectra of all the complexes were recorded in CH_2Cl_2 solution at 298 K and are gathered in Fig. 7. All spectra display intense $\pi\rightarrow\pi^*$ ligand-centred (LC) transitions in the near UV region and metal-to-ligand-charge-transfer (MLCT) bands in the range 320-400 nm. The MLCT features of the homoleptic species $[Cu(N\text{^}N)_2]^+$ are at higher energy with respect to those of similar Cu(I)-bisphenantroline-type complexes, such as $[Cu(dmp)_2]^+$ (where dmp is 2,9-dimethyl-1,10-phenanthroline),[7a] probably as a consequence of the reduced size ring of the tetrazole group that enhances the energy of the π^* accepting orbital. In the case of the heteroleptic species, dppe and POP-based complexes display relatively well resolved MLCT transitions centred at 380 and 350 nm, respectively, while those of $[Cu(N\text{^}N)(dppm)]^+$ lie at higher energy ($\lambda_{max} \approx 320$ nm) as a shoulder of the LC features.

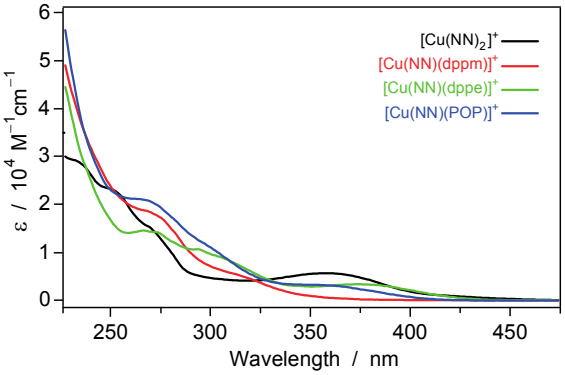

Fig. 7. Room-temperature absorption spectra in CH_2Cl_2 solution. Experimental measurements were made at concentrations between 10^{-5} and 10^{-6} M where dimeric species are negligible (*vide infra*).

While the homoleptic complex $[Cu(N\text{^}N)_2]^+$ is not emissive both in CH_2Cl_2 solution and in solid matrices, the heteroleptic complexes exhibit emission bands attributable to deactivations from triplet excited MLCT levels (^{3}MLCT*); photoluminescence data are collected in Table 6. In CH_2Cl_2 solution, only $[Cu_n(N\text{^}N)_n(dppm)_n]^{n+}$ (n=1,2) and $[Cu(N\text{^}N)(POP)]^+$ are luminescent weak and structureless emission at 578 and 582 nm, respectively. These compounds exhibit singlet-oxygen sensitized emission in air-equilibrated solutions at about 1270 nm and this corroborates the triplet nature of the emitting states.[21] A dramatically different behaviour is observed in the solid state, where all the heteroleptic complexes exhibit intense emissions both in CH_2Cl_2 frozen matrix at 77 K (Fig. 8) and at room temperature in KBr pellets or in PMMA thin films (Figs. 9 and 10, respectively). Although the emission intensity at 77 K can be hardly evaluated quantitatively, a bright green luminescence is observed for all the heteroleptic complexes upon UV excitation (Xe lamp, 150 W). Emission spectra at 77 K are red-shifted compared to 300 K, as typically observed

for $[Cu(NN)(PP)]^+$ complexes[6g]., and related excited state lifetimes are long (0.15-0.25 ms, Table 6).

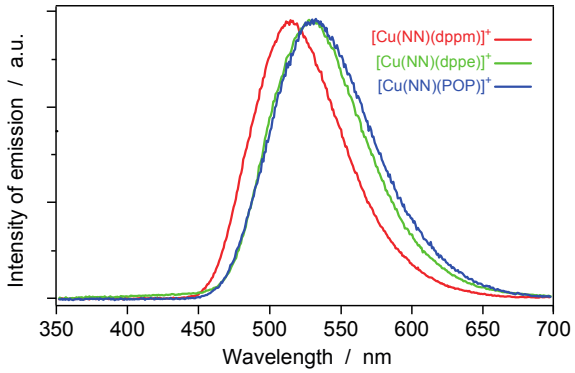

Fig. 8. Normalized emission spectra in CH_2Cl_2 rigid matrix at 77 K (λ_{exc} = 280 nm).

In RT solid matrices all the heteroleptic complexes, particularly the dimeric form of $[Cu(N^N)(dppm)]^+$, show bright and long-lived photoluminescence ($\tau \approx 20$ μs and Φ up to 45%, in KBr). It has to be noted that the highest PLQYs in KBr pellets, compared to those in PMMA films (Figs.9-10, Table 6), can be attributed to the fact that the preparation process of polymeric films requires the solubilisation of the sample, followed by spin casting, a procedure that may cause decomposition to some extent.

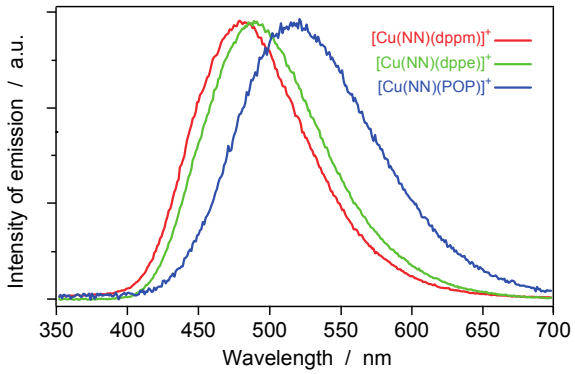

Fig. 9. Normalized emission spectra in KBr pellets at room temperature (λ_{exc} = 280 nm).

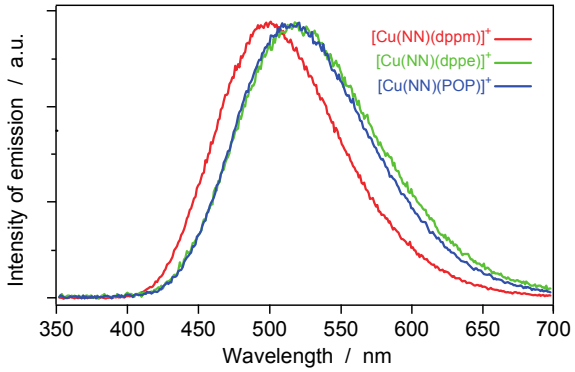

Fig. 10. Normalized emission spectra in PMMA thin films at room temperature (λ_{exc} = 280 nm).

Table 6 Luminescence data of all the complexes under different experimental conditions

Complex	RT CH_2Cl_2		KBr pellets			PMMA films			77 K rigid matrix	
	$\lambda^{[a]}$ [nm]	$\Phi^{[b,c]}$ [%]	$\lambda^{[a]}$ [nm]	$\tau^{[d]}$ [μs]	$\Phi^{[b,e]}$ [%]	$\lambda^{[a]}$ [nm]	$\tau^{[d]}$ [μs]	$\Phi^{[b,e]}$ [%]	$\lambda^{[a]}$ [nm]	$\tau^{[d]}$ [μs]
$[Cu(NN)_2]^+$	[f]	[f]	[f]	[f]	[f]	[f]	[f]	[f]	[f]	[f]
$[Cu(NN)(dppm)]^+$	578	< 0.1	484	4.9 (15%) 21.5 (85%)	45	495	2.8 (16%) 12.7 (84%)	35	510	150
$[Cu(NN)(dppe)]^+$	[f]	[f]	493	4.3 (13%) 21.8 (87%)	34	515	0.8 (17%) 5.5 (83%)	6	528	240
$[Cu(NN)(POP)]^+$	582	< 0.1	532	3.3 (33%) 19.5 (67%)	14	515	0.8 (10%) 6.3 (90%)	17	530	260

[a] Emission maxima from uncorrected spectra. [b] λ_{exc} = 280 nm. [c] In oxygen-free solution; standard used, $[Ru(bpy)_3]^{2+}$ in air-equilibrated water (Φ = 0.028). [d] Determined using the single-photon-counting technique; λ_{exc} = 278 nm (laser diode). [e] Determined using integrating sphere. [f] Not emissive.

Conclusions

N-alkylated tetrazoles can be considered as diimine analogues for the design of homoleptic Cu-based compounds of the type $[Cu(N^N)_2]^+$ and for mixed ligands complexes of the general formula $[Cu(N^N)(P^P)]^+$, where P^P represents a chelating diphosphine. Interestingly, by means of NMR spectroscopy and X-ray diffraction, it has been possible to evidence that $[Cu(N^N)(dppm)]^+$ and $[Cu(N^N)(dppe)]^+$ preferentially adopt a dimeric structure in which the diphosphines act as the bridge between two metal centers. Although all the investigated complexes are poorly luminescent in dichloromethane solution at room temperature, heteroleptic complexes $[Cu(N^N)(dppm)]^+$, $[Cu(N^N)(dppe)]^+$ and $[Cu(N^N)(POP)]^+$ exhibit high quantum yields and emission lifetimes in the range 3-22 μs in KBr matrix at room temperature. These features suggest that heteroleptic complexes with tetrazole ligands are potentially exploitable to design cheap emitting materials for LEECs-type devices based on copper.

Experimental Section

Materials. All reactions were routinely carried out under Argon atmosphere, using standard Schlenk techniques. Solvents were distilled immediately before use under nitrogen from appropriate drying agents. Unless otherwise stated, chemicals were obtained commercially (*e.g.* Aldrich) and used without further purification. $[Cu(CH_3CN)_4][BF_4]$,[13] and 2-(1,H-tetrazol-5-yl)pyridine[22]were prepared according to literature methods. Throughout this paper, the percentage yields of the product complexes are referred to the molar quantity of the starting $[Cu(CH_3CN)_4][BF_4]$.

Warning! Tetrazole derivatives are used as components for explosive mixtures.[23] In this lab, the reactions described here were only run on a few gram scale and no problems were encountered. However, great caution should be exercised when handling or heating compounds of this type.

Instrumentation and procedures. All the obtained complexes were characterized by elemental analysis and spectroscopic methods. Elemental analyses were performed on a ThermoQuest Flash 1112 Series EA instrument. Mass spectra were performed on a Waters ZQ-4000 instrument (ESI-MS, acetonitrile as the solvent). The routine NMR spectra (^1H, ^{13}C, ^{31}P) were always recorded using a Varian Mercury Plus 400 instrument (^1H, 400.1; ^{13}C, 101.0; ^{31}P, 162.0 MHz). The spectra were referenced internally to residual solvent resonance, and were recorded at 298 K for characterization purposes. Relative to the description of the ^1H and ^{13}C NMR spectra (see further on), the atom numbering is always referred to Scheme 2.

Electrochemistry. Tetrabutylammonium hexafluorophosphate (TBAH; from Fluka), as supporting electrolyte, was used as received. Dry dichloromethane (DCM) was purified and dried as previously reported,[24] stored in a specially designed Schlenk flask and protected from light. Shortly before performing the experiment, the solvent was distilled via a closed system into an electrochemical cell containing the supporting electrolyte and the species under examination. Electrochemical experiments were carried out in an airtight single-compartment cell described elsewhere[25] by using platinum and glassy carbon as working electrode, a platinum spiral as counter electrode and a silver spiral as a quasi-reference electrode. The cell containing the supporting electrolyte and the electroactive compound was dried under vacuum at about 110 °C for at least 60 h before each experiment. All the $E_{½}$ potentials have been directly obtained from CV curves as averages of the cathodic and anodic peak potentials for one-electron peaks and by digital simulation for those processes closely spaced in multielectron voltammetric peaks. The $E_{½}$ values are referred to an

aqueous saturated calomel electrode (SCE) and have been determined by adding, at the end of each experiment, ferrocene as an internal standard and measuring them with respect to the ferrocinium/ferrocene couple standard potential. The potentials thus obtained were not corrected for the two unknown contribution of the liquid junction potential between the organic phase and the aqueous SCE solution. Voltammograms were recorded with a custom made fast potentiostat controlled by an AMEL model 568 programmable function generator. The potentiostat was interfaced to a Nicolet model 3091 digital oscilloscope and the data were transferred to a personal computer by the program *Antigona*.[26] The minimization of the uncompensated resistance effect in the voltammetric measurements was achieved by the positive-feedback circuit of the potentiostat. Digital simulations of the cyclic voltammetric curves were carried out either by Antigona or DigiSim 3.0. The determination of the potentials, for the irreversible processes, and the heterogeneous electron transfer constant were obtained by digital simulation of the cyclic voltammetric curves utilizing a best fitting procedure of the experimental curves recorded at different scan rates spanning over, at least, two orders of magnitude.

Photophysics. Spectroscopic investigations were carried out in CH_3CN and CH_2Cl_2 (Carlo Erba, spectrofluorimetric grade), used without further purification. Absorption spectra were recorded with a Perkin-Elmer Lambda 950 spectrophotometer. For photoluminescence experiments, the samples were placed in fluorimetric 1 cm-path Suprasil quartz cuvettes and purged from oxygen by bubbling with argon. Uncorrected emission spectra were obtained with an Edinburgh FLS920 spectrometer equipped with a Peltier-cooled Hamamatsu R928 photomultiplier tube (185−850 nm). An Edinburgh Xe900 450 W xenon arc lamp was used as the excitation light source. Corrected spectra were obtained via a calibration curve supplied with the instrument. The apparatus for the determination of the singlet oxygen luminescence in the near-infrared region has been described elsewhere.[27] Photoluminescence quantum yields (Φ_{PL} or PLQY) in solution were obtained from corrected spectra on a wavelength scale (nm) and measured according to the approach described by Demas and Crosby[28] using air-equilibrated $[Ru(bpy)_3][Cl]_2$ water solution (Φ_{PL} = 0.028)[29] as standard. Emission lifetimes (τ) were measured with an IBH single photon counting spectrometer equipped with a pulsed NanoLED excitation source (λ_{exc} at 278 nm; pulse width ≤ 0.3 ns); the detector was a red-sensitive (185–850 nm) Hamamatsu R-3237-01 PMT. Analysis of the luminescence decay profiles was accomplished with the DAS6 Decay Analysis Software provided by the manufacturer and the quality of the fit was assessed by the χ^2 value close to unity with the residuals regularly distributed along the time axis. To record the 77 K luminescence spectra, the samples were put in quartz tubes (2 mm inner diameter) and inserted in a special quartz Dewar flask

filled up with liquid nitrogen. Solid samples were prepared following two different procedures: the PMMA films containing 25% wt. of the complex were drop-cast from dichloromethane solutions; the KBr pellets were obtained by grinding the solid sample with solid potassium bromide purchased from Sigma-Aldrich, ACS reagent. The thickness of the polymeric films was not controlled; the sample concentration in the KBr pellet was depending on the absorption coefficient of each complex. Solid-state Φ_{PL} values were calculated by corrected emission spectra obtained from an Edinburgh FLS920 spectrometer equipped with a barium sulfate-coated integrating sphere (diameter of 4 in.) following the procedure described by De Mello et al.[30] Experimental uncertainties are estimated to be ±8% for τ determinations, ±20% for PLQYs, ±2 nm and ±5 nm for absorption and emission peaks, respectively.

Ligand synthesis

The ligand 2-(2-*tert*-butyl-tetrazol-5-yl)pyridine (N^N) was prepared by following a literature method that involves the addition of a 0.500 g (3.40 mmol) aliquot of 2(1,H-tetrazol-5-yl)pyridine to 25 mL of tert-butanol in the presence of 3.0 mL of trifluoroacetic acid and 3.0 mL of concentrated sulphuric acid. The mixture was left to stir at r.t. overnight, during which time the initial suspension turned to a yellowish solution. Then, the mixture was poured into ice-water and made alkaline (pH>12) by the addition of KOH pellets. The resulting mixture was extracted with chloroform (3x15 mL) and the organic layers were dried over $MgSO_4$. The solvent was then removed by rotary evaporation, providing the desired compound (0.370 g, 54%) as an oily yellow residue. m.p.: 73-74°C. ^{1}H NMR ($CDCl_3$, 400 MHz, r.t.) 8.78 (d, J = 5.0 Hz , 1H, H_6), 8.25 (d, J = 8.0 Hz, 1H, H_3,), 7.83 (t, J = 8.0 Hz, 1H, H_4), 7.37-7.34 (m, 1H, H_5), 1.81 (s, 9H, C-(CH_3)$_3$) ppm; ^{13}C NMR ($CDCl_3$, 101 MHz, r.t.) 164.6 (Ct), 150.6 (C_6), 147.6 (Ci), 137.3 (C_4), 124.9 (C_3), 122.8 (C_5), 64.8 (*C*-(CH$_3$)$_3$), 29.8 (C-(*C*H$_3$)$_3$) ppm.

Synthesis of the homoleptic complex [Cu(N^N)$_2$][BF$_4$]:

[Cu(CH$_3$CN)$_4$][BF$_4$] (0.315 g, 1.0 mmol) was dissolved in 20 mL of dichloromethane in a 100 mL Schlenck tube protected from light and under an Argon atmosphere. Then, 5.0 mL of a dichloromethane solution containing 0.406 g (2.0 mmol, 2 equiv.) of 2-(2-*tert*-butyl-2*H*-tetrazol-5-yl)pyridine (N^N) was added dropwise over a period of 30 minutes. Once the addition was completed, the mixture was left to stir at r.t. for 1 hour, after which time the total volume was reduced to ca. 5.0 mL. The subsequent slow diffusion of diethyl ether (ca. 20.0 mL) into the concentrated dichloromethane solution induced the formation of white-yellowish crystals of [Cu(N^N)$_2$][BF$_4$] suitable for X-ray diffraction analysis. Yield 87%. ESI-MS (*m/z*) = 469 [M-

$BF_4]^+$. ^{1}H NMR (400 MHz, $CDCl_3$, r.t) 8.67 (br, 1H, H_6), 8.29 (br, 1H, H_3,), 8.15 (br, 1H, H_4), 7.74 (br, 1H, H_5), 1.82 (br, 9H, C-(C*H*$_3$)$_3$); ^{13}C NMR ($CDCl_3$ 101 MHz, r.t): 163.4 (Ct), 150.7 (C_6), 143.9 (C_i), 139.9 (C_4), 128.4 (C_3), 122.8 (C_5), 67.2 (*C*-(CH_3)$_3$), 29.5 (C-(*C*H_3)$_3$). Anal. Calcd. for $C_{20}H_{26}BCuF_4N_{10}$ (556.17): C, 43.15; H, 4.71; N, 25.18. Found: C, 43.11; H, 4.75; N, 25.22 %.

Synthesis of the heteroleptic complexes [Cu(N^N)(P^P)][BF$_4$]

[Cu(CH_3CN)$_4$][BF_4] (0.315 g, 1.0 mmol) was dissolved in 20 mL of dichloromethane in a 100 mL Schlenck tube protected from light and under an Argon atmosphere. Once the Cu(I) salt was completely dissolved, 1.0 mmol (1 equiv.) of the appropriated diphosphine was added to the solution. The mixture was left to stir at r.t. for 2 hours, after which time 5.0 mL of a dichloromethane solution containing 0.203 g (1.0 mmol, 1 equiv.) of 2-(2-*tert*-butyl-2*H*-tetrazol-5-yl)pyridine (N^N) was added dropwise over a period of 30 minutes. After two hours of stirring at r.t., the solvent was removed in vacuo until the total volume was reduced to ca. 5.0 mL. Then, the subsequent slow diffusion of diethyl ether (ca. 20.0 mL) into the concentrated dichloromethane solutions induced the formation of white crystals of desired mixed ligand complexes which were found as suitable for X-ray diffraction analysis. In the only case of the dppe-based complex, the batches deriving from the crystallization procedure were contaminated by small amounts of the homoleptic byproduct [Cu(dppe)$_2$][BF_4]. This impurity could be efficiently removed by performing two to three successive recrystallization from the same CH_2Cl_2/Et_2O mixtures.

[Cu$_2$(N^N)$_2$(dppm)$_2$][BF$_4$]$_2$: Yield 75%; ESI-MS (*m/z*) = 650 [M – BF_4]$^+$ and [M_2 -2BF_4]$^{2+}$. ^{1}H NMR (400 MHz, $CDCl_3$, r.t): 8.49 (br, 2H, H_6), 7.71 (br, 6H, H_3 + H_4 + H_5), 7.23-6.75 (br, 40 H, Ph-dppm), 3.70 (br, 4H, C*H*$_2$-dppm), 1.84 (br, 18H, C-(C*H*$_3$)$_3$); ^{1}H NMR: (400 MHz, $CDCl_3$, 233.15 K) 8.49 (br, 2H, H_6), 8.01 (br, 2H, H_3), 7.82 (br, 2H, H_4), 7.58 (br, 1H, H_5), 7.15-6.84 (br, 40H, Ph-dppm), 3.60 (br, 4H, C*H*$_2$-dppm) 1.92 (s, 8H C-(C*H*$_3$)$_3$), 1.83 (s, 10H, C-(C*H*$_3$)$_3$);^{13}C NMR: (101 MHz, $CDCl_3$) 162.3 (Ct), 151.0 (C_6), 142.6 (Ci), 138.8 (C_4), 132.7-127.5 (phenyls-dppm and C_3), 122.3 (C_5), 67.4 (*C*-(CH_3)$_3$), 29.6 (C-(*C*H_3)$_3$), 26.2 (*C*H_2-dppm); ^{31}P NMR (162 MHz, $CDCl_3$, r.t.) -7.0 (s) ppm. Anal. Calcd. for [Cu_2(N^N)$_2$(DPPM)$_2$][BF_4]$_2$, $C_{70}H_{70}B_2Cu_2F_8N_{10}P_4$ (1474.34): C, 56.97; H, 4.79; N, 9.50. Found: C, 56.95; H, 4.74; N, 9.51 %.

[Cu$_2$(N^N)$_2$(dppe)$_2$][BF$_4$]$_2$: Yield 71%; ESI-MS (*m/z*) = 664 [M – BF_4]$^+$; ^{1}H NMR (400 MHz, $CDCl_3$) 8.35-.17 (m, 6H, H_6 + H_3 + H_4) 7.66-7.62 (m, 2H, H_5), 7..37-7.30 (m, 40 H, phenyls-dppe), 2.51-2.49 (m, 8H, C*H*$_2$-dppe), 1.83 (s, 18H, C-(C*H*$_3$)$_3$); ^{13}C NMR (101 MHz, CDCl3): 163.0 (Ct), 150.9 (C_6), 143.9 (Ci), 140.3 (C_4), 132.9, 131.2, 130.75, 129.9, 129.4 (dppe), 128.3 (C_3), 123.67

(C_5), 66.2 (*C*-(CH_3)$_3$, 29.7 (C-(*C*H_3)$_3$), 26.4 (*C*H_2-dppe); ^{31}P NMR (162 MHz, CDCl3) -4.25 (s) ppm. Anal. Calcd. for [Cu_2(N^N)$_2$(DPPE)$_2$][BF_4]$_2$·Et_2O, $C_{76}H_{84}B_2Cu_2F_8N_{10}OP_4$ (1576.44): C, 57.85; H, 5.37; N, 8.88. Found: C, 57.92; H, 5.40; N, 8.91 %.

[Cu(N^N)(POP)][BF_4]: Yield 85%; ESI-MS (*m/z*) = 804 [M – BF_4]$^+$. ^{1}H NMR: (400 MHz, $CDCl_3$, r.t.) 8.37-8.24 (m, 2H, H_6 + H_3), 8.20 (d, 1H, H_4), 7.58 (m, 1H, H_5), 7.44-7.33 (m, 16H, POP), 7.12-7.08 (m, 4H, POP), 6.91-6.88 (m, 4H, POP), 1.83 (s, 9H, C-(C*H*$_3$)$_3$); ^{13}C NMR: (101 MHz, $CDCl_3$, r.t.) 162.46 (Ct), 158.6 (POP), 150.1 (C_6), 143.6 (Ci), 140.3 (C_4), 134.5, 132.5, 130.8, 129.1, 127.9, (POP), 125.4,(C_3), 123,7, 123.38 (POP), 120.7 (C_5), 67.1 (*C*-(CH_3)$_3$), 29.6 (C-(*C*H_3)$_3$); ^{31}P NMR (162 MHz, $CDCl_3$) -11.2 (s) ppm. Anal. Calcd. for [Cu(N^N)(POP)][BF_4]·Et_2O, $C_{50}H_{51}BCuF_4N_5O_2P_2$ (965.28): C, 62.16; H, 5.32; N, 7.25. Found: C, 62.15; H, 5.35; N, 7.22 %.

X-ray crystallography. Crystal data and collection details for [Cu(N^N)$_2$][BF_4], [Cu_2(N^N)$_2$(DPPM)$_2$][BF4]$_2$, [Cu_2(N^N)$_2$(DPPE)$_2$][BF_4]$_2$·Et_2O and [Cu(N^N)(POP)][BF_4]·Et_2O are reported in Table 7. The diffraction experiments were carried out on a Bruker APEX II diffractometer equipped with a CCD detector and using Mo-Kα radiation. Data were corrected for Lorentz polarization and absorption effects (empirical absorption correction SADABS).[31] Structures were solved by direct methods and refined by full-matrix least-squares based on all data using F^2.[32] H-atoms were placed in calculated positions, and refined isotropically using the 1.2 fold U_{iso} value of the parent atom except methyl protons, which were assigned the 1.5 fold U_{iso} value of the parent C-atom. All non-hydrogen atoms were refined with anisotropic displacement parameters. Similar *U* restraints were applied to the C and F atoms of [Cu_2(N^N)$_2$(DPPM)$_2$][BF_4]$_2$ (s.u. 0.005), and to the C atoms of [Cu(N^N)(POP)][BF_4]·Et_2O (s.u. 0.01). The [BF_4]$^-$ anion in [Cu(N^N)(POP)][BF_4]·Et_2O is disordered, and therefore it has been split into two positions and refined isotropically using one occupancy parameter per disordered group. Restraints to bond distances in [Cu(N^N)(POP)][BF_4]·Et_2O were applied (s.u. 0.01) to the Et_2O molecule: 1.53 Å for C–C and 1.43 Å for C–O. The crystals of [Cu_2(N^N)$_2$(DPPE)$_2$][BF_4]$_2$·Et_2O had a quite low diffraction power and this accounts for a higher value of R(int) (21.51%). Even in this structure the [BF_4]$^-$ anion is disordered and therefore has been split in two positions in the refinement, using distance and anisotropic displacement parameter restraints. Bond distances comparable to those cited above and *U* restraints were also employed for the disordered Et_2O solvent molecule.

Acknowledgements. This work was supported by MIUR (PRIN 2008) and the CNR (PM.P04.010, MACOL).

Table 7

Crystal data and collection details for $[Cu(N^N)_2][BF_4]$, $[Cu_2(N^N)_2(dppm)_2][BF4]_2$, $[Cu_2(N^N)_2(dppe)_2][BF_4]_2{\cdot}Et_2O$ and $[Cu(N^N)(POP)][BF_4]{\cdot}Et_2O$

	$[Cu(N^N)_2][BF_4]$	$[Cu_2(N^N)_2(dppm)_2][BF_4]_2$	$[Cu_2(N^N)_2(dppe)_2][BF_4]_2{\cdot}Et_2O$	$[Cu(N^N)(POP)][BF_4]{\cdot}Et_2O$
Formula	$C_{20}H_{26}BCuF_4N_{10}$	$C_{70}H_{70}B_2Cu_2F_8N_{10}P_4$	$C_{76}H_{84}B_2Cu_2F_8N_{10}OP_4$	$C_{50}H_{51}BCuF_4N_5O_2P_2$
Fw	556.86	1475.94	1578.11	966.25
T, K	100(2)	292(2)	296(2)	296(2)
λ, Å	0.71073	0.71073	0.71073	0.71073
Crystal system	Orthorhombic	Monoclinic	Triclinic	Monoclinic
Space Group	$P2_12_12_1$	$C2/c$	$P\bar{1}$	$P2_1$
a, Å	9.647(2)	42.896(3)	11.935(5)	9.8303(7)
b, Å	12.310(3)	13.8035(10)	12.949(5)	21.6994(15)
c, Å	21.399(4)	24.5456(17)	14.490(6)	11.6696(8)
α, °	90	90	73.001(5)	90
β, °	90	99.2160(10)	68.107(5)	94.9510(10)
γ, °	90	90	88.574(5)	90
Cell Volume, Å^3	2541.2(9)	14346.2(18)	1978.2(14)	2480.0(3)
Z	4	8	1	2
D_c, g cm^{-3}	1.454	1.367	1.325	1.294
μ, mm^{-1}	0.918	0.751	0.686	0.563
F(000)	1144	6080	818	1004
Crystal size, mm	0.25×0.21×0.15	0.21×0.16×0.12	0.20 x 0.15 x 0.12	0.18×0.15×0.11
θ limits, °	1.90–28.00	1.55–27.00	1.59 to 25.00	1.75–27.00
Index ranges	-12≤ h ≤ 12 -15≤ k ≤ 15 -28≤ l ≤ 28	-54≤ h ≤ 54 -17≤ k ≤ 17 -31≤ l ≤ 31	−14 ≤ h ≤ 14 −15 ≤ k ≤ 15 −17 ≤ l ≤ 17	-12≤ h ≤ 12 -27≤ k ≤ 27 -14≤ l ≤ 14
Reflections collected	29121	78301	18689	27802

Independent reflections	6031 [R_{int} = 0.0268]	15663 [R_{int} = 0.0580]	6952 [R(int) = 0.2151]	10836 [R_{int} = 0.0531]
Completeness to θ max	99.0	100.0%	99.7 %	100.0%
Data / restraints / parameters	6031 / 0 / 332	15663 / 426 / 865	6952 / 211 / 536	10836 / 388 / 553
Goodness on fit on F^2	1.042	1.046	0.917	0.989
R_1 ($I > 2\sigma(I)$)	0.0313	0.0593	0.0811	0.0646
wR_2 (all data)	0.0896	0.1943	0.2121	0.2087
Absolute structure parameter	0.973(9)	-	0.521 and –0.440	0.01(2)
Largest diff. peak and hole, e $Å^{-3}$	0.840 / –0.347	0.847 / –0.511	521 and –0.440	0.620 / –0.524

References

1 a) H. Yersin, Ed.; Highly Efficient OLEDs with Phosphorescent Materials; Wiley-VCH: Weinheim, Germany, 2008; b) L. Xiao, Z. Chen, B. Qu, J. Luo, S. Kong, Q. Gong, J. Kido, *Adv. Mater.*, 2011, **23**, 926-952 and references cited therein.

2 a) C. Adachi, M. A. Baldo, M. E. Thompson, S. R. Forrest, *J. Appl. Phys.*, 2001, **90**, 5048; b) M. A. Baldo, S. Lamansky, P. E. Burrows, M. E. Thompson, S. R. Forrest, *Appl. Phys. Lett.* 1999**, 75**, 4-6; c) M. A. Baldo, D. F. O'Brien, Y. You, A. Shoustikov, S. Sibley, M. E. Thompson, S. R. Forrest, *Nature* 1998, **395**, 151–154; see also: d) H. Yersin, A. F. Rausch R. Czerwieniec, T. Hofbeck, T. Fischer, *Coord. Chem. Rev.* 2011, **255**, 2622-2652, and references cited therein.

3 L. Flamigni, A. Barbieri, C. Sabatini, B. Ventura, F. Barigelletti, *Top. Curr. Chem.*, 2007, **281**, 143-203, and references cited therein.

4 a) C.H. Yang, J. Beltran, V. Lemaur, J. Cornil, D. Hartmann, W. Sarfert, R. Frolich, C. Bizzarri, L. De Cola, *Inorg. Chem.,* 2010, **49**, 9891-9901; b) M. Cocchi, J. Kalinowski, S. Muzzioli, S. Stagni, *Appl. Phys. Lett.,* 2009, **94**, 083306; c) C.-F. Chang, Y.-M. Cheng, Y. Chi, Y.-C. Chiu, C.-C. Lin, G.-H. Lee, P.-T. Chou, C.-C. Chen, C.-H. Chang, C.-C. Wu, *Angew. Chem. Int. Ed.,* 2008, **47**, 4542-4545; d) E. Orselli, G. S. Kottas, A. E. Konradsson, P. Coppo, R. Frohlich, L. De Cola, A. van Dijken, M. Buchel, H. Borner, *Inorg. Chem.,* 2007, **46**, 11082-11093; e) P.-T. Chou, Y. Chi, *Chem. Eur. J.,* 2007, **13**, 380-395; f) E. Holder, B. M. W. Langeveld, U. S. Schubert, *Adv. Mater.,* 2005, **17**, 1109-1121, and references cited therein.

5 a) A. Barbieri, G. Accorsi, N. Armaroli, *Chem. Commun.* 2008, 2185-2193 and references cited therein; see also: b) G. F. Manbeck, W. W. Brennessel, R. Eisenberg, *Inorg. Chem.,* 2011, **50**, 3431-3441;

6 a) Q. Zhang, Q. Zhou, Y. Cheng, L. Wang, D. Ma, X. Jing F. Wang, *Adv. Mater.*, 2004, **16**, 432-436 ; b) R. D. Costa, D. Tordera, E. Orti, H. J. Bolink, J. Schonle, S. Graber, C. E. Housecroft, E. C. Constable, J. A. Zampese, *J. Mater. Chem.,* 2011, **21**, 16108-16118. c) J. C. Deaton, S. C. Switalski, D. Y. Kondakov, R. H. Young, T. D. Pawlik, D. J. Giesen, S. B. Harkins, A. J. M. Miller, S. F. Mickenberg, J. C. Peters, *J. Am. Chem. Soc.,* 2010, **132**,

9499-9508; d) L. M. Zhang, B. Li, Z. M. Su, *J. Phys. Chem. C.,* 2009, **113**, 13968-13973; e) A. Tsuboyama, K. Kuge, M. Furugori, S. Okada, M. Hoshino, K. Ueno, *Inorg. Chem.,* 2007, **46**, 1992-2001; f) O. Moudam, A. Kaeser, A. Delavaux-Nicot, C. Duhayon, M. Holler, G. Accorsi, N. Armaroli, I. Seguy, J. Navarro, P. Destruel, J. F. Nierengarten, *Chem. Commun.,* 2007, 3077-3079; g) N. Armaroli, G. Accorsi, M. Holler, O. Moudam, J. F. Nierengarten, Z. Zhou, R. T. Wegh, R. Welter, *Adv. Mater.,* 2006, **18**, 1313-1316.

7 a) N. Armaroli, G. Accorsi, F. Cardinali, A. Listorti, *Top Curr. Chem.* 2007, **280**, 69-115 and references cited therein; see also: b) G. Accorsi, N. Armaroli, C. Duhayon, A. Saquet, B. Delavaux-Nicot, R. Welter, O. Moudam, M. Holler, J.-F. Nierengarten, *Eur. J. Inorg. Chem.* 2010, 164-173; c) A. Lavie-Cambot , M. Cantuela, Y. Leydet, G. Jonusauskas, D. M. Bassani, N. D. McClenaghan, *Coord. Chem. Rev.*, 2008, **252**, 2572-2584.

8 a) R. Czerwieniec, J. Yu, H. Yersin, *Inorg. Chem.,* 2011, **50**, 8293-8301; b) U. Monkowius, S. Ritter, B. König, M. Zabel, H. Yersin, *Eur. J. Inorg. Chem.,* 2007, 4597-4606; c) S.-H. Kuang, D. G. Cuttell, D. R. McMillin, P. E. Fanwick, R. A. Walton, *Inorg. Chem.,* 2002, **41**, 3313-3322; d) D. G. Cuttell, S.-H. Kuang, P. E. Fanwick, D. R. McMillin, R. A. Walton, *J. Am. Chem Soc.* 2002, **124**, 6-7.

9 a) S. Stagni, A. Palazzi, P. Brulatti, M. Salmi, S. Muzzioli, S. Zacchini, M. Marcaccio, F. Paolucci, *Eur. J. Inorg. Chem.* 2010, 4643-4657; b) S. Stagni, E. Orselli, A. Palazzi, L. De Cola, S. Zacchini, C. Femoni, M. Marcaccio, F. Paolucci, S. Zanarini, *Inorg. Chem.* 2007, **46**, 9126-9138; c) S. Stagni, A. Palazzi, S. Zacchini, B. Ballarin, C. Bruno, M. Marcaccio, F. Paolucci, M. Monari, M. Carano, A. J. Bard, *Inorg. Chem.* 2006, **45**, 695-709; d) S. Zanarini, A. J. Bard, M. Marcaccio, A. Palazzi, F. Paolucci, S. Stagni, *J. Phys. Chem. B* 2006, **110**, 22551-22556; e) M. Duati, S. Tasca, F. C. Lynch, H. Bohlen, J. G. Vos, S. Stagni, M. D. Ward, *Inorg. Chem.* 2003, **42**, 8377-8384; f) M. Massi, M. Cavallini, S. Stagni, A. Palazzi, F. Biscarini, *Mat. Sci. Eng. C*, 2003, **23**, 923-925.

10 S. Stagni, S. Colella, A. Palazzi, G. Valenti, S. Zacchini, F. Paolucci, M Marcaccio, R. Q. Albuquerque, L. De Cola, *Inorg. Chem.,* 2008, **47**, 10509-10521.

11 M. V. Werrett, D. Chartrand, G. D. Gale, G. S. Hanan, J. G. MacLellan, M. Massi, S. Muzzioli, P. Raiteri, B. W. Skelton, M. Silberstein, S. Stagni, *Inorg. Chem.,* 2011, **50**, 1229-1241.

12 A. J. Downard, P. J. Steel, J. Steenwijk, *Aust. J. Chem.,* 1995, **48**, 1625-1642.

13 G. J. Kubas, *Inorg. Synth.,* 1979, **19**, 90.

14 a) P. W. N. M. van Leeuwen, P. C. J. Kamer, J. N. H. Reek, P. Dierkes, *Chem. Rev.,* 2000, **100**, 2741-2770; b) L. A. van der Veen, P. K. Keeven, G. C. Schoemaker, J. N. H. Reek,; P. C. J. Kamer, P. W. N. M. van Leeuwen, M. Lutz, A. L. Spek, *Organometallics,* 2000, **19**, 872-883.

15 a) P. C. J. Kamer, P. W. N. M. van Leeuwen, J. N. H. Reek *Acc. Chem. Res.* 2001, **34**, 895-904; b) M. Kranenburg, Y. E. M. van der Burgt, P. C. J. Kamer, P. W. N. M. van Leeuwen, K. Goubitz, K. Fraanje, *Organometallics* 1995, **14**, 3081-3089.

16 a) Y. Chen, J.-S. Chen, X. Gan, W.-F. Fu, *Inorg. Chim. Acta*, 2009, **362**, 2492-2498; b) Y. Sun, S. Zhang, G Li, Y. Xie, D. Zhao, *Transition Met. Chem.,* 2003, **28**, 772-776; c) Y.-Q. Wei, K.-C. Wu, Z.-F. Zhuang, *J. Coord. Chem.,* 2006, **59**, 713-719; d) Q.-H. Wei, G.-Q.Yin, L.-Y. Zhang, Z.-N. Chen, *Inorg. Chem.* 2006, **45**, 10371-10377.

17 a) R. D. Adams, B. Captain, Q.-F. Zhang, *Z. Anorg. Allg. Chem.,* 2007, **633**, 2187-2190; b) R. N.; Yang, D. M.Wang, Y. F.Liu,; D. M. Jin, *Polyhedron,* 2001, **20**, 585-590.

18 a) J. Guerrero, L. Cortez, L. Lemus, L. Farías, J. Costamagna, C. Pettinari, M. Rossi, F. Caruso, *Inorg. Chim. Acta*, 2010, **363**, 3809-3816; b) I. I. Vorontsov, T. Graber, A. Yu. Kovalevsky, I. V. Novozhilova, M. Gembicky, Yu-S. Chen, P. Coppens, *J. Am. Chem. Soc.*, 2009, **131**, 6566-6573; c) T. M^{c}Cormick, W.-L. Jia, S. Wang, *Inorg. Chem.*, 2006, **45**, 147-155; d) P. Coppens, I. I. Vorontsov, T. Graber, A. Yu. Kovalevsky, Y.-S. Chen, G. Wu, M. Gembick, I. V. Novozhilova, *J. Am. Chem. Soc.,* 2004, **126**, 5980-5981; e) P. Coppens, *Chem. Commun.,* 2003, 1317-1320.

19 K. Saito, T. Arai, N. Takahashi, T. Tsukuda, T. Tsubomura, *Dalton Trans.,* 2006, 4444-4448.

20 Q. Zhang, Q. Zhou, Y. Cheng, L. Wang, D. Ma, X. Jing, F. Wang, *Adv. Funct. Mater* 2006, **16**, 1203-1208; L. Yang, J.-K. Feng, A.-M. Ren, M. Zhang, Y.-G. Ma, X.-D. Liu, *Eur. J. Inorg. Chem.,* 2005, **44**, 1867-1879.

21 J.-M. Kern, J.-P. Sauvage, J.-L. Weidmann, N. Armaroli, L. Flamigni, P. Ceroni, V. Balzani, *Inorg. Chem.*, 1997, **36**, 5329-5338.

22 W. G. Finnegan, R. A. Henry, R. Lofquist, *J. Am. Chem. Soc.,* 1958, **80**, 3908-3911.

23 R.N. Butler, Tetrazoles. In "*Comprehensive Heterocyclic Chemistry II*"; Storr, R. C., Ed.; Pergamon Press: Oxford, U.K., 1996; Vol. 4, pp 621-678, and references cited therein.

24 C. Bruno, I. Doubitski, M. Marcaccio, F. Paolucci, D. Paolucci, A. Zaopo *J. Am. Chem. Soc.* 2003, **125**, 15738-15739.

25 M. Marcaccio, F. Paolucci, C. Paradisi, M. Carano, S. Roffia, C. Fontanesi, L. J. Yellowlees, S. Serroni, S. Campagna, V. Balzani, *J. Electroanal. Chem.* 2002, **532**, 99-112.

26 a) Antigona is a program developed by Dr. Loïc Mottier, University of Bologna, Bologna, Italy, 1999; b) B. Spieser in Electroanalytical Chemistry. A Series of Advances, vol. 19 (Eds: A. J. Bard, I. Rubistein), Marcel Dekker, Inc., New York, 1996, p.1.

27 N. Armaroli, G. Accorsi, F. Song, A. Palkar, L. Echegoyen, D. Bonifazi, F. Diederich, *ChemPhysChem*, 2005, **6**, 732–743

28 G. A. Crosby, J. N. Demas, *J. Phys. Chem.,* 1971**, 75**, 991-1024.

29 K. Nakamaru, *Bull. Chem. Soc. Jpn.,* 1982**, 55**, 2697-2705.

30 J. C. De Mello, H. F. Wittmann, R. H. Friend, *Adv. Mater.,* 1997**, 9**, 230-236.

31 G. M. Sheldrick, , SADABS, Program for Empirical Absorption Correction, University of Göttingen, Germany, 1996.

32 G.M. Sheldrick, SHELX97-Program for the refinement of Crystal Structure, University of Göttingen, Germany, 1997

New Tetrazole-based Cu(I) Homo- and Heteroleptic Complexes with Various Diphosphine Ligands: Synthesis, Characterization and Study of their Redox and Photophysical Properties

Cristina Femoni,[a] Sara Muzzioli,[a] Antonio Palazzi,[a] Stefano Stagni,[a]* Stefano Zacchini,[a] Filippo Monti,[b] Gianluca Accorsi,[b] Margherita Bolognesi,[b] Nicola Armaroli,[b]* Massimiliano Massi,[c] Giovanni Valenti,[d] Massimo Marcaccio[d]

Graphical contents entry

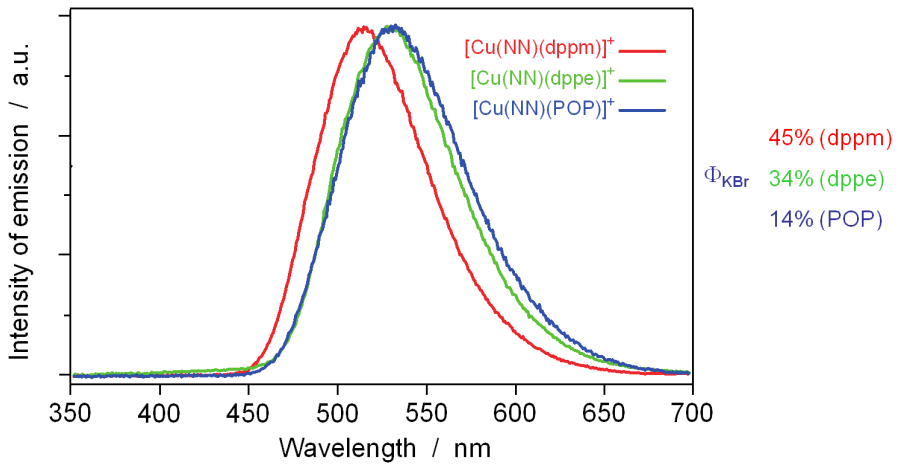

Four new cationic Cu(I) complexes containing an aromatic N-alkylated tetrazole as the diimine type ligand (N^N) and various chelating diphosphines (P^P) have been prepared and fully characterized. The mixed ligand species $[Cu_n(P\hat{}P)_n(N\hat{}N)_n]^{n+}$ (n=1,2) display bright green photoluminescence in the solid state at r.t., reaching quantum yield values up to 45%.